

MODELLING THE EFFECTS OF SURCHARGE TO REDUCE LONG TERM SETTLEMENT OF RECLAMATIONS OVER SOFT CLAYS: A NUMERICAL CASE STUDY

DAVID NASH¹⁾

ABSTRACT

Long-term settlement of reclamations constructed over soft soils may be reduced by the use of temporary pre-loading, although there is often uncertainty over how much surcharge to use, and how long it should be maintained. An elastic visco-plastic constitutive model is described and its application in assessing surcharging strategy for reclamation schemes is discussed. The model is incorporated in a one-dimensional finite difference consolidation analysis with vertical and radial drainage of a multi-layer soil profile. The analysis allows the inclusion of vertical drain resistance, a zone of peripheral smear around the drain, permeabilities that vary with void ratio, and creep both during and after primary consolidation. Drawing on data from the Bothkennar soft clay research site, the model is used to predict settlements beneath a hypothetical test fill, including the creep settlement behaviour when a surcharge is removed after different time periods. The behaviour during primary consolidation is back-analysed using Asaoka's and the hyperbolic observational methods, and both are found to under-predict the magnitude of the settlement.

Key words: consolidation, creep, finite difference analysis, preloading, reclamation, soft clay, surcharge, vertical drains (IGC: D5/E13)

INTRODUCTION

Construction of reclamations over compressible soils frequently necessitates the use of ground improvement techniques to accelerate their consolidation and minimise post-construction settlements. Vertical drains are often installed to accelerate consolidation, and may be either sand columns constructed by jetting, boring or displacement techniques, or prefabricated band drains. When post-construction settlements are likely to be significant due to lack of full pore pressure dissipation or creep, it is common to attempt to reduce these by application of a temporary surcharge to pre-load the ground over critical areas. Earth fill is generally used to provide the surcharge but other techniques such as the vacuum method or water loading are sometimes adopted.

The principles for compensating for primary consolidation are well established (Johnson, 1970), but partial compensation for secondary consolidation is harder to achieve with confidence (Bjerrum, 1972). Procedures for determining the rate and magnitude of secondary compression after surcharge removal are not well established. Generally predictions are made using empirical relationships between the coefficient of secondary compression C_{α} for normally consolidated clay and that for the over-

consolidated clay (Jamiolkowski et al., 1983; Holtz et al., 1991; Mesri et al., 1994). These authors acknowledge the difficulty of predicting settlement rates in subsoils exhibiting creep, and especially when the surcharge is removed.

Similar problems are encountered in designing surcharge to embankments built on soft clays. Nash and Ryde (1999; 2001) have recently developed numerical procedures for analysing the consolidation of a soft soil adjacent to a vertical drain to explore the effects of creep, and applied them in the back-analysis of the performance of some embankments built over estuarine alluvium in the UK. The finite strain analysis includes the effects of non-linear stiffness, creep, and permeability varying with void ratio as well as drain resistance and smear around the vertical drain. A simple isotache constitutive model originally proposed by Yin and Graham (1989; 1994 and 1996) was adopted, and subsequently the author has developed this to include more features of a structured clay. In this paper the newer constitutive models are described and the application of the procedures to reclamation projects is discussed. These are illustrated by predictions of the behaviour of the soft clay beneath fill hypothetically placed at the Bothkennar soft clay research site.

¹⁾ Department of Civil Engineering, University of Bristol, Bristol BS8 1TR, UK.
Manuscript was received for review on July 21, 2000.

Written discussions on this paper should be submitted before May 1, 2002 to the Japanese Geotechnical Society, Sugayama Bldg. 4F, Kanda Awaji-cho 2-23, Chiyoda-ku, Tokyo 101-0063, Japan. Upon request the closing date may be extended one month.

MODELLING CREEP IN SOFT CLAYS

Background

The first theory of secondary compression was formulated by Taylor and Merchant (1940) and since then straining under constant effective stresses has been an area of continual study. They showed that secondary compression movements decrease logarithmically with time, and Taylor (1948) stated that creep occurs during primary consolidation as well as subsequently. Following Taylor's ideas, Suklje (1957) and Bjerrum (1967) presented diagrams showing a system of approximately parallel e vs. $\log \sigma'$ curves (see Fig. 1) that describe secondary compression behaviour. In this widely used diagram, the lines indicate void ratio or strain after constant time for delayed compression. Bjerrum introduced the terms instant and delayed compression to describe the behaviour of the soil skeleton in the absence of hydrodynamic effects, and argued that delayed compression (or creep) occurs during the whole consolidation process. Bjerrum (1972) developed these concepts when discussing the use of temporary surcharge to reduce long-term movements, and drew attention to the significance of secondary compression for the design of vertical drain installations. He showed that although improved drainage accelerates primary consolidation, it does not affect the magnitude of total long-term settlement.

Creep at constant effective stress is usually described using the secondary compression index $C_{\alpha} = \Delta e / \Delta \log t$ but there has always been difficulty in deciding the time ori-

gin. The main area of debate (Ladd et al., 1976; Jamiolkowski et al., 1983; Mesri and Choi, 1985a; Leroueil, 1988) has been whether creep is significant during primary consolidation. If creep only commences after primary consolidation is complete (hypothesis A), the end of primary (EOP) e vs. $\log \sigma'$ curve is practically independent of the thickness of the compressible stratum and the duration of primary consolidation. If creep is significant both during and after primary compression (hypothesis B), field and laboratory stress-strain behaviour will be different.

Mesri and Choi (1985b) developed the finite difference procedure ILLICON that utilises Hypothesis A, and the assumption is made that the secondary compression index C_{α} is linearly related to the compression index C_c (Mesri and Godlewski, 1977). Subsequently ILLICON was extended to include flow into a vertical drain, and experience of its use was summarised by Mesri et al. (1994).

Bjerrum's ideas (Hypothesis B) were expressed mathematically by Garlanger (1972), and Magnan et al. (1979) used a stress-strain-strain rate model in the one-dimensional consolidation analysis CONMULT. Kabbaj et al. (1986) proposed separating elastic and plastic components of strain, and subsequently Yin and Graham (1989; 1994 and 1996) and Den Haan (1996) developed similar elastic visco-plastic (EVP) models that overcome some of the previous limitations. These elastic visco-plastic (EVP) models avoid the difficulty of determining the time origin for creep since creep rate is determined directly using isotaches, but while they have been used successfully in modelling laboratory data, there is little published on their application to full-scale problems. In selecting a model for use in back-analysis of the performance of embankments built over soft clay, Nash and Ryde (1999; 2001) concluded it was desirable to model creep during primary consolidation (hypothesis B), and adopted the EVP model of Yin and Graham as the starting point for their work. In this paper the model is developed further to enable a structured soft clay to be modelled.

Simple Isotache Model for One-Dimensional Compression

Yin and Graham (1989) used the λ - κ model from critical state soil mechanics to define the one-dimensional elastic-plastic behaviour of the soil skeleton. In their model the normal consolidation line (NCL) is replaced by a reference time line (RTL), as illustrated in Fig. 2. On this diagram the parallel lines or isotaches connect soil states at which the creep strain rate is constant. One isotache on which the creep strain rate is known is chosen as the RTL, which is used to define the complete set of isotaches; equally spaced isotaches indicate a logarithmic change in strain rate. The creep strain rate is uniquely defined by the current state of the soil—hence it is a simple isotache model (Tatsuoka et al., 1999).

The solid line ABD in Fig. 2 indicates a path that might be followed by an element of soil loaded by an increment of total stress $\Delta \sigma$ as it consolidates one-dimensionally. At any state the total strain of the soil skeleton

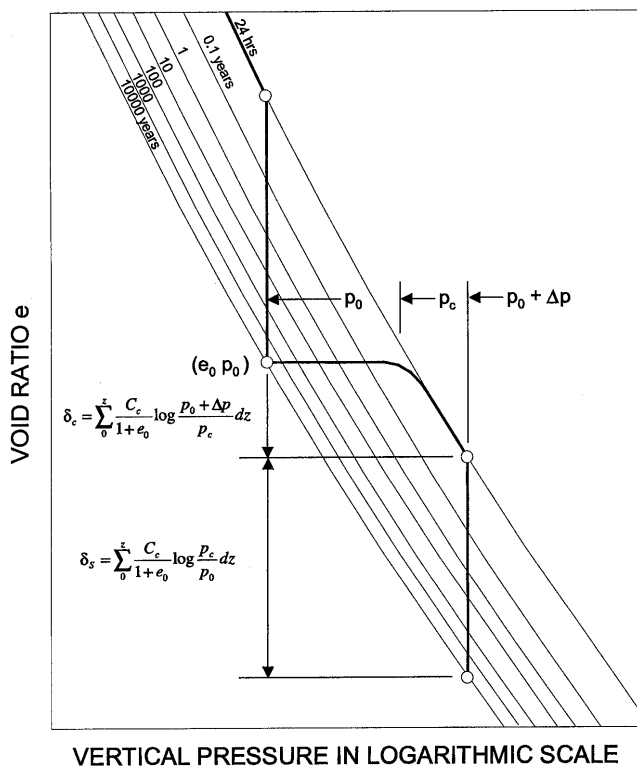


Fig. 1. Principle for evaluating secondary settlements in soft clay (Bjerrum, 1967)

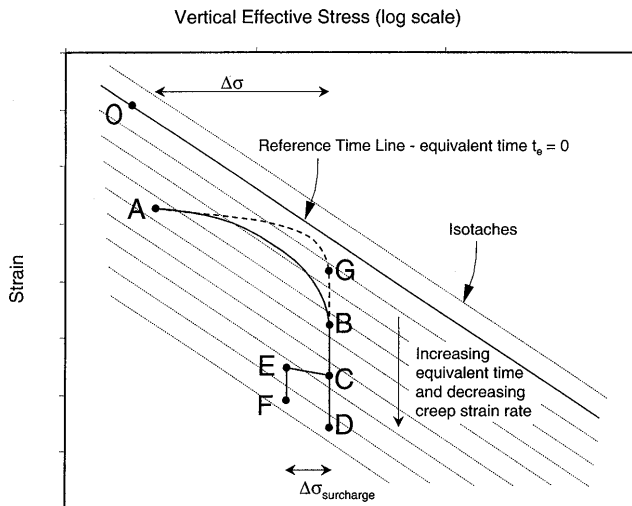


Fig. 2. Elastic visco-plastic constitutive model showing isotaches and stress-strain path during consolidation and subsequent creep behaviour

is the sum of the elastic strain and the creep or time-dependent strain. As the effective stress increases from the initial state at point A, the creep strain rate increases as the soil state moves towards the RTL, but the effective stress and strain rate are limited by the ability of the porewater to escape. After further consolidation the strain rate decreases until excess pore pressures have dissipated at point B, after which creep continues at decreasing rates towards point D. If the loading is reduced with a consequential reduction of effective stress say from C to E the creep rate is reduced to that of the corresponding isotache at E. Thereafter creep continues at a reduced rate towards point F.

It is important to realise that the stress strain behaviour of each element in the ground during primary consolidation will be different depending on its proximity to a drainage boundary. A soil element remote from a drainage boundary may follow the path AB indicated by the solid line whilst another element closer to the drainage boundary might consolidate faster, with the path from A to B lying closer to the RTL as shown by the dashed line. For this element the end of primary consolidation occurs at point G. Indeed a small sample of the soil subjected to the same loading in an oedometer might follow a path which crossed the RTL.

In the EVP model of Yin and Graham (1989)—herein denoted model 1—the RTL₁ (with the subscript indicating model 1) is linear on a semi-logarithmic plot of specific volume v (or engineering strain ε) vs. effective stress. The RTL₁ has slope λ (or the combination λ/v_0 where v_0 is the specific volume at zero strain), and is fixed by the stress¹ σ_1^{ep} and the corresponding specific volume v_1^{ep} (or engineering strain $\varepsilon_1^{\text{ep}}$) at a reference state O (see Fig. 2). The equation of the RTL₁ is thus:

$$v^{\text{ep}} = v_1^{\text{ep}} - \lambda \ln \left(\frac{\sigma'}{\sigma_1^{\text{ep}}} \right) \quad \text{or the equivalent}$$

$$\varepsilon^{\text{ep}} = \varepsilon_1^{\text{ep}} + \frac{\lambda}{v_0} \ln \left(\frac{\sigma'}{\sigma_1^{\text{ep}}} \right). \quad (1)$$

The model may be used to describe many aspects of the behaviour of soft clays pertinent to reclamation projects. Since the creep rate is uniquely defined by the current state of the soil, the model may be used to predict the behaviour in unloading as well as loading. However the model also has several limitations. Firstly, the isotaches are linear on a plot of specific volume (or engineering strain) vs. $\log \sigma'$, but in practice structured clays frequently exhibit curved normal consolidation lines. Secondly the separation of the isotaches is constant whereas tests show that at high stresses the separation of the isotaches decreases. Thirdly there is no lower limit to creep and under small applied loading the model may predict unrealistically high creep rates.

These problems may be partially overcome if natural strain, herein denoted $\bar{\varepsilon}$, is considered (following Butterfield, 1979) rather than engineering strain, herein denoted ε , where natural strain is defined as:

$$\bar{\varepsilon} = - \int_{v_0}^v \frac{dv}{v} = - \ln \left(\frac{v}{v_0} \right) = - \ln (1 - \varepsilon) \quad (2)$$

in which v is the specific volume as before and v_0 is its value at the start of straining. Butterfield showed that for many natural clays a plot of natural strain or logarithm of specific volume against logarithm of vertical effective stress is more linear than the usual semi-logarithmic plot of engineering strain vs. effective stress.

A second model (denoted model 2) has been developed by the author which is formulated in terms of natural strain instead of engineering strain. The RTL₂ has a slope λ^*/v_0 where v_0 is the specific volume at zero strain as before, and it is fixed by the stress σ_2^{ep} and the corresponding specific volume v_2^{ep} or natural strain $\bar{\varepsilon}_2^{\text{ep}}$ at a reference state O (see Fig. 2—here with natural strain as ordinate). The equation of the RTL₂ is given by:

$$\ln (v^{\text{ep}}) = \ln (v_2^{\text{ep}}) - \frac{\lambda^*}{v_0} \ln \left(\frac{\sigma'}{\sigma_2^{\text{ep}}} \right)$$

or the equivalent

$$\bar{\varepsilon}^{\text{ep}} = \bar{\varepsilon}_2^{\text{ep}} + \frac{\lambda^*}{v_0} \ln \left(\frac{\sigma'}{\sigma_2^{\text{ep}}} \right). \quad (3)$$

The incremental total strain $\partial \bar{\varepsilon}$ resulting from a change of vertical effective stress $\partial \sigma'$ is the sum of the incremental elastic strain $\partial \bar{\varepsilon}^e$ and the incremental creep strain $\partial \bar{\varepsilon}^{\text{tp}}$ given by Eq. (4):

$$\partial \bar{\varepsilon} = \partial \bar{\varepsilon}^e + \partial \bar{\varepsilon}^{\text{tp}} = \frac{\kappa^*}{v_0 \sigma'} \partial \sigma' + \partial \bar{\varepsilon}^{\text{tp}} \quad (4)$$

where σ' is the current vertical effective stress and κ^*/v_0 is the slope of the elastic unload-reload line (natural strain $\bar{\varepsilon}^e$ vs. $\ln \sigma'$). The creep strain rate is defined by the relation of the current soil state to the RTL₂ through the introduction of the concept of equivalent time t_e . This is

¹The super-scripts *e*, *ep* and *tp* denote instantaneous (elastic), stress-dependent plastic and time-dependent plastic, respectively.

the time which would be taken to creep under constant effective stress from the RTL_2 (where t_e is zero) to the present state. Thus the parallel isotaches on Fig. 2 are t_e isochrones. It is easier to understand the model if the chosen RTL_2 is located above the normal consolidation line, but this is not a requirement as t_e may assume negative values providing that $t_e > -t_0$.

The creep strain rate is calculated from the expression:

$$\dot{\bar{\epsilon}}^{tp} = \frac{\partial \bar{\epsilon}^{tp}}{\partial t} = \frac{\psi^*}{v_0(t_0 + t_e)} \quad (5)$$

in which ψ^*/v_0 is the slope of a plot of creep strain $\bar{\epsilon}^{tp}$ vs. $\ln(t_e)$ (similar to the conventional coefficient of secondary consolidation C_α), and t_0 is used to define the creep rate on the RTL_2 . It follows that the difference in strain between the current state and that on the RTL_2 at the same stress is given by:

$$\Delta \bar{\epsilon}^{tp} = \frac{\psi^*}{v_0} \ln \left(1 + \frac{t_e}{t_0} \right). \quad (6)$$

By combining Eqs. (5) and (6) it follows that when the soil creeps at constant effective stress:

$$\Delta \bar{\epsilon}^{tp} = \frac{\psi^*}{v_0} \left(\ln \left(\frac{\psi^*}{v_0 t_0} \right) - \ln(\dot{\bar{\epsilon}}^{tp}) \right). \quad (7)$$

When Eq. (6) is combined with the Eq. (3) for the RTL , the total strain is given by:

$$\bar{\epsilon} = \bar{\epsilon}_2^{sp} + \frac{\lambda^*}{v_0} \ln \left(\frac{\sigma'}{\sigma_2'^{sp}} \right) + \frac{\psi^*}{v_0} \ln \left(1 + \frac{t_e}{t_0} \right). \quad (8)$$

This expression can be rearranged so that the equivalent time may be calculated from:

$$t_e = -t_0 + t_0 \exp \left[(\bar{\epsilon} - \bar{\epsilon}_2^{sp}) v_0 / \psi^* \right] \times \left(\frac{\sigma'}{\sigma_2'^{sp}} \right)^{-\lambda^*/\psi^*}. \quad (9)$$

Equation (9) contains the ratio ψ^*/λ^* which is similar to the more usual C_α/C_c . It is inherent in this model that the ratio ψ^*/λ^* remains constant along the isotaches (in line with the findings of Mesri and Godlewski, 1977), which leads to some convergence of the isotaches at high stresses on a semi-logarithmic plot of engineering strain vs. effective stress.

In some structured clays even the curvature of the reference time line implied by model 2 may not provide a good match to the data. Further curvature of the isotaches may be introduced by using a power formulation for the RTL . A third EVP model—herein denoted model 3—has been developed in a similar manner to model 2 described above, in which the creep natural strain rate and the ratio ψ/λ (in engineering strain) are maintained constant along the RTL_3 . Adopting a form similar to that proposed by Den Haan (1992) specific volume is related to its value at a reference state² ($\sigma_3'^{ep}$, v_3^{sp}) given by:

$$\ln(v^{ep}) = \ln(v_3^{sp}) - b \ln(\sigma' - (\sigma_3'^{ep} - 1)) \quad (10)$$

in which the parameter b controls the curvature of the isotaches. The RTL_3 is asymptotic to a stress of $(\sigma_3'^{ep} - 1)$ at large specific volume. A full description of this model will be given elsewhere.

Obtaining Model Parameters

The model parameters may be obtained from high quality incremental load oedometer tests. Using a plot of natural strain $\bar{\epsilon}$ vs. $\log \sigma'$, a linear RTL_2 is chosen that passes through points of constant creep strain rate, approximately parallel to the normal consolidation line. Yin and Graham (1994) suggest an iterative procedure to locate the RTL above the NCL , particularly when load increments are applied after variable time intervals. However the author has found that in many oedometer tests with increments applied daily, the strain rate after 24 hours is approximately constant in the normally consolidated stress range. The 24 hour line may then be used directly as the RTL_2 , and its position defined by choosing a reference state. In many instances it is convenient to project the RTL back to zero strain. Values of λ^* and κ^* are found from the slopes of the chosen RTL_2 and the unloading/reloading curves respectively, and the remaining parameters are found from the creep data. The parameter ψ^* may readily be obtained from the slope of plots of logarithm of strain rate against strain for the later stages of each increment using Eq. (7); a single value is required that most closely matches the data in the stress range of interest. The value of t_0 is then calculated from the creep rate on the RTL .

In practise it has been found convenient to define the reference time lines for all three models using a common state ($\sigma_1'^{ep}$, ϵ_1^{ep} or v_1^{ep}) at which the positions of the reference time lines coincide, and the slopes $\partial v^{ep}/\partial \sigma'$ and $\partial v^{tp}/\partial t$ are equal. Starting from a conventional plot of void ratio or engineering strain vs. $\log \sigma'$, the RTL_1 is located approximately parallel to the normal consolidation line and its position fixed using the chosen common state as the reference state. The parameters λ , κ and ψ for model 1 are obtained in a manner similar to that described above. The reference state for model 2 ($\sigma_2'^{ep}$, v_2^{sp}) is chosen coincident with ($\sigma_1'^{ep}$, v_1^{ep}), and the parameters for model 2 are obtained by calculation using the equations below (see Appendix for derivation):

$$\lambda^* = \frac{\lambda v_0}{v_1}, \quad \kappa^* = \frac{\kappa v_0}{v_1}, \quad \psi^* = \frac{\psi v_0}{v_1}. \quad (11)$$

With model 3, to achieve coincidence of the RTL_3 with that of the other models at the common state ($\sigma_1'^{ep}$, v_1^{ep}) a different reference state ($\sigma_3'^{ep}$, v_3^{sp}) is chosen (see Appendix) which is defined by:

$$\begin{aligned} \sigma_3'^{ep} &= \sigma_1'^{ep} \left(1 - \frac{b v_1^{ep}}{\lambda} \right) + 1, \\ v_3^{sp} &= v_1^{ep} \left(\frac{b v_1^{ep} \sigma_1'^{ep}}{\lambda} \right)^{-b}. \end{aligned} \quad (12)$$

The creep parameters for model 3 are not central to this paper and their derivation will be presented elsewhere.

²Den Haan used symbols v_1 to denote the specific volume at the reference state and $p_s = \sigma_3' - 1$, but these are changed here for clarity.

The implementation of these EVP models in a finite difference consolidation analysis is described in the next section, and their use in assessing the effectiveness of surcharge in reducing long-term settlements is described later in the paper.

FINITE DIFFERENCE PROCEDURE

Consolidation Equation

The analysis of consolidation with vertical drains is generally based on the axisymmetric one-dimensional consolidation equation (Terzaghi, 1943) in which the three-dimensional process of consolidation is simplified to that of one-dimensional movement arising from a combination of vertical flow and radial flow to the drain. This equation is often written:

$$c_v \frac{\partial^2 \bar{u}}{\partial z^2} + c_r \left(\frac{\partial^2 \bar{u}}{\partial r^2} + \frac{1}{r} \frac{\partial \bar{u}}{\partial r} \right) = \frac{\partial \bar{u}}{\partial t} \quad (13)$$

in which \bar{u} is the excess pore pressure and c_v and c_r are the vertical and radial coefficients of consolidation respectively. Barron (1948) and Hansbo (1981) obtained closed form solutions for equal strain (in which the surface displacements are constant but the applied stress is non-uniform), and Barron also considered free strain (in which the applied vertical stress at the surface remains constant and settlements are non-uniform). They also considered the important practical problems of smear around the drain and drain resistance effects. Such solutions necessitate the simplifying assumptions made by Terzaghi, including that the vertical and horizontal coefficients of consolidation c_v and c_r remain constant during consolidation and that the relationship between void ratio and effective stress is linear and independent of time. In addition it must be assumed that the applied load remains constant during consolidation, that deformations are small compared to the original geometry and are one-dimensional, and that boundary pore-pressure conditions remain constant. These assumptions are not valid for the consolidation of thick layers of soft clay in which a significant proportion of the compression is due to creep, and closed form solutions are not available.

The consolidation equation is generally expressed in terms of excess pore pressure \bar{u} on the assumption that the steady-state pore pressure u_{ss} remains constant. The terms involving \bar{u} are derived from total head h and position head z where:

$$h = \frac{u}{\gamma_w} + z = \frac{\bar{u} + u_{ss}}{\gamma_w} + z. \quad (14)$$

If the boundary conditions may change, it is convenient to use the full pore pressure u with an additional term on the left-hand side of the consolidation equation to account for the variation of pressure with elevation. Equation (13) may then be written:

$$\frac{\partial}{\partial z} \left(\frac{k_z}{\gamma_w} \left(\frac{\partial u}{\partial z} + \gamma_w \right) \right) + \frac{1}{r} \frac{\partial}{\partial r} \left(\frac{k_r}{\gamma_w} r \frac{\partial u}{\partial r} \right)$$

$$= m_v \left(\frac{\partial u}{\partial t} - \frac{\partial \sigma}{\partial t} \right) + \frac{\partial \bar{\epsilon}^{vp}}{\partial t} \quad (15)$$

where k_z and k_r are hydraulic conductivities in vertical and radial directions, and m_v is the coefficient of volume compressibility. If the boundary pore pressures do not change the equation may be expressed in terms of excess pore pressure \bar{u} and the extra term involving γ_w is omitted. The variation of total vertical stress σ with time, and creep are taken into account by inclusion of additional terms on the right hand side, which express the elastic and plastic components of natural strain rate. The soil may be modelled as linear elastic (using a constant m_v) or non-linear (by varying m_v with stress level), with or without creep.

Finite Difference Formulation

In order to model the consolidation of layered soil profiles due to vertical and radial flow, Eq. (15) has been expressed in implicit finite difference form³ (Ryde, 1997; Nash and Ryde, 2001). The solution has been implemented in a procedure termed BRISCON using Visual Basic for Excel, with data held on worksheets, permitting graphs to be plotted conveniently.

The use of finite difference methods for the analysis of consolidation problems is well established in the geotechnical literature (for example Richart, 1959; Murray, 1971; Olsen et al., 1974; Lee et al., 1983 and Onoue, 1988). However Ryde (1997) adopted a numerical formulation technique different from that previously used, similar to that developed by Reece (1986) in the analysis of heat flow through a non-uniform metal bar. The soil is divided into a series of layers and annuli as shown in Fig. 3. The grid is graded in both directions so that there are small layer and annulus thicknesses close to permeable boundaries. The state of the soil in each cell is represented by the conditions at a central node, which is positioned so that the cell boundaries lie mid-way between adjacent nodes. This contrasts with previous consolidation analyses in which the nodes were generally positioned at the cell boundaries.

Phantom nodes and layers are placed just outside the boundaries of the grid to enable the boundary conditions to be defined. At the start of the analysis the steady state conditions are determined by iteration with the right hand side of Eq. (15) set to zero. These pore pressures are used to determine the initial distribution of effective stress. As the analysis proceeds the coordinates are updated, with the values of soil bulk density, permeability, stiffness and creep rate being those applicable to the current soil state. With increasing settlement the applied loading may change due to partial submergence of the fill, and also the boundary conditions change as noted by Olsen and Ladd (1979). By updating the boundary pore pressures during the analysis this effect is taken into account, since the pore pressures obtained in the solution

³Originally, Ryde (1997) formulated Eq. (15) in terms of excess pore pressure.

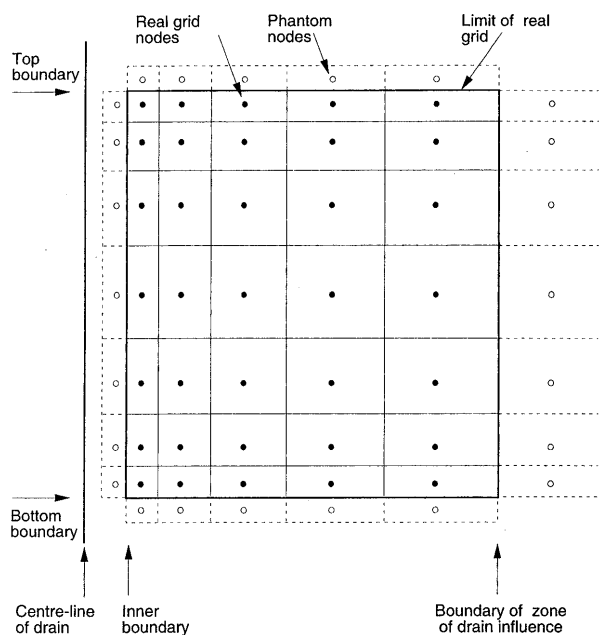


Fig. 3. Grid used in finite difference analysis

converge to the long-term steady state values.

While free drainage is often assumed at the vertical drain, the effects of drain resistance may be modelled explicitly by incorporating the drain within the grid. The drain annulus is given equivalent discharge capacity and an impermeable core, and the terms on the right-hand side of Eq. (15) for the relevant cells are set to equal zero.

To simulate an equal strain condition the total stresses applied at ground level may be redistributed using an iterative procedure. During development, BRISCON was used to analyse some simple problems. Comparison was made with closed form solutions (Barron, 1948) and with solutions obtained using the finite element program CRISP; in all cases satisfactory agreement was obtained. Details of the finite difference procedure and its validation are given in Ryde (1997) and Nash and Ryde (2001).

CASE STUDY

The EVP models outlined above have been used in the BRISCON procedure to predict the behaviour of the clay at the Bothkennar soft clay research site in Scotland if a wide fill were placed. This site was chosen because the clay was the subject of an extensive collaborative research programme undertaken in the early 1990s and the ground conditions are well described in a series of papers (Géotechnique, 1992). The post-glacial organic estuarine silty clay at Bothkennar is of high plasticity, and its sensitivity from vane tests averages about 5. A desiccated crust 2 m thick overlies about 16 m of lightly over-consolidated soft clay (OCR about 1.6), beneath which is a layer of dense sand and gravel. Groundwater conditions are hydrostatic below 0.8 m depth. The reader is referred to Géotechnique (1992) for further details.

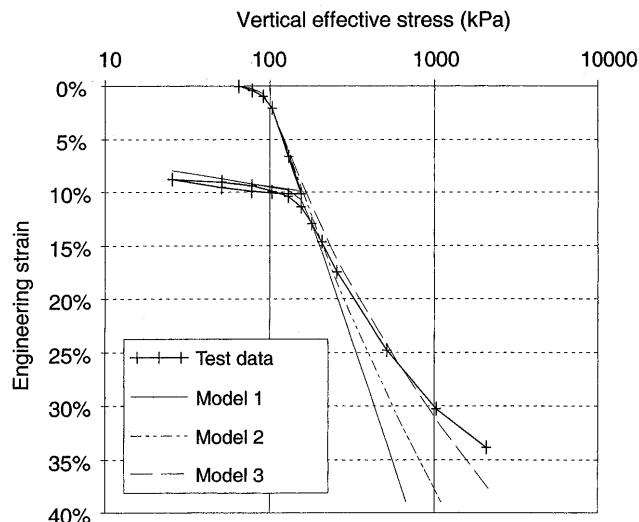


Fig. 4. Data from IL test 16B-3: Experimental stress-strain behaviour and results predicted by BRISCON

Compressibility and Permeability of Bothkennar Clay

During the characterisation study a large number of oedometer tests were carefully undertaken on samples obtained with the Laval or Sherbrooke samplers (Nash et al., 1992), comprising 45 incremental load (IL), 24 constant rate of displacement and 13 restricted flow tests. Each IL test involved 20 to 30 load increments, which were generally applied daily. A typical loading sequence utilised four equal load increments up to the in-situ vertical effective stress. Then small load increments of around 10 kPa were used to define the yield stress, after which larger increments with a load-increment ratio of 1 were applied to a maximum stress of around 2000 kPa. Some tests were run with extended load increments, and many had unload-reload loops. Recently the data were re-examined to determine compressibility and creep parameters for use with the EVP models.

An example of the test data is given in Fig. 4, which shows data from a sample (16B-3) taken from half way down the profile. On a plot of engineering strain versus logarithm of effective stress, a line was carefully drawn tangent to the first part of the curved normal consolidation line. This line was chosen as the RTL_1 , and its position was fixed by determining the stress at 1% strain and its slope. Here the origin used for strain was taken after recompression to the in-situ stress. Creep parameters were derived using Eq. (7) from plots of strain against logarithm of strain rate. Figure 5 shows the data from test 16B-3 for the three increments either side of yield plotted in this way. It may be seen that the slopes vary, increasing to yield and then decreasing, and the maximum value was usually selected. Figure 5 also shows that the creep rates at the end of each increment after yield were generally similar at about 0.03%/hour. This uniformity of strain rate justifies selecting a RTL coincident with the 24-hour normal consolidation line.

Using the data obtained from this test a check was made that the observed behaviour could be predicted

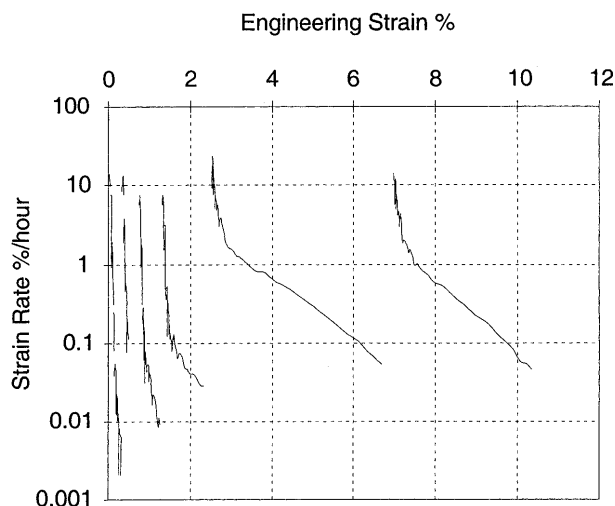


Fig. 5. Creep data from IL test 16B-3

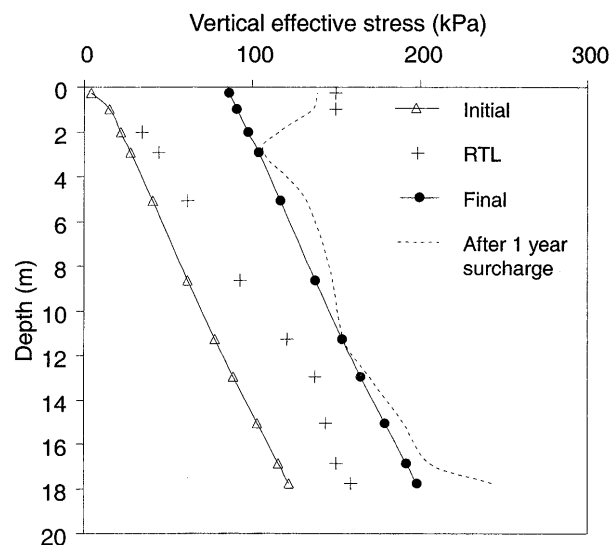


Fig. 6. Profiles of vertical effective stresses

satisfactorily using model 1 with BRISCON. The results of a complete simulation of this test are shown alongside the experimental data in Fig. 4, with the data plotted for the end of each load increment. It may be seen that for stresses around yield there is good agreement. While the model correctly predicts the swelling on unloading and creep when the previous maximum stress is approached, it does not predict the hysteresis observed in practice. It should be noted that creep occurs throughout consolidation, so during each increment the stress-strain path lies above the RTL. Load increments of longer duration would of course result in larger strains. At high stresses this model over-predicts the changes of void ratio, because the RTL_1 is linear.

Better agreement is obtained using model 2, with parameters chosen so that the RTL_2 gradient was matched to that of the linear RTL_1 at the common point. Values were first obtained for the parameters λ , κ and ψ , and these were then directly related to λ^* , κ^* and ψ^* through Eqs. (11) as discussed above. A similar procedure was followed for model 3, which provides an even better fit at high stresses. For clarity the unload-reload loop is only shown for the EVP model 1.

The data from all the IL tests have been examined in a similar manner and soil parameters obtained for the whole profile. The reference stresses are related to the ini-

tial in-situ vertical effective stress by a ratio similar to the yield stress ratio (except for the crust for which a constant value was chosen). The strain rate on the RTL was taken as 0.03%/hour over the full depth. Data on the permeability of the silty clay are based on those reported by Hight et al. (1992) in their Table 6, and the horizontal permeability is typically 1.5 times greater than the vertical permeability. As the clay is compressed the permeability reduces with void ratio, according to:

$$\Delta \log k = \Delta e / C_k \quad (16)$$

where C_k is the permeability change index. Although Hight et al. (1992) indicate that taking C_k equal to half the natural void ratio as suggested by Tavenas et al. (1983) slightly overestimates C_k for Bothkennar clay, the value $C_k = 0.5e_0$ has been assumed here for both vertical and horizontal permeability.

The soil parameters are summarised in Table 1.

Numerical Study

In this study the effects of placing fill equivalent to 100 kPa on the ground surface with and without vertical drains and temporary surcharge have been simulated using BRISCON. Except where noted the analyses used the EVP model 2, with continuous updating of the geome-

Table 1. Soil parameters derived from IL oedometer tests on Bothkennar clay

Layer	Thickness	γ kN/m ³	e_0	$\frac{\sigma_1^{ep}}{\sigma_1^{ep} \text{ or } \sigma'_0}$	ϵ_1^{ep}	λ^*	κ^*	ψ^*/λ^*	RTL strain rate %/hr	k_v , m/sec	k_h , m/sec
Crust	1.5 m	16.87	1.100	150	1%	0.137	0.014	0.03	0.03	$1.0 \times 10^{-9\dagger}$	$1.0 \times 10^{-9\dagger}$
Soft silty clay	2.5 m	16.38	1.750	1.6	1%	0.362	0.024	0.04	0.03	1.0×10^{-9}	1.1×10^{-9}
Soft silty clay	3.0 m	15.60	1.950	1.5	1%	0.453	0.030	0.04	0.03	1.2×10^{-9}	1.9×10^{-9}
Soft silty clay	3.0 m	15.77	1.800	1.5	1%	0.491	0.032	0.04	0.03	9.3×10^{-10}	1.1×10^{-9}
Soft silty clay	4.0 m	16.21	1.700	1.55	1%	0.509	0.033	0.04	0.03	5.7×10^{-10}	6.4×10^{-10}
Soft silty clay	2.0 m	16.73	1.550	1.4	1%	0.425	0.028	0.04	0.03	3.6×10^{-10}	8.6×10^{-10}
Soft silty clay	2.0 m	17.10	1.350	1.3	1%	0.309	0.021	0.04	0.03	$2.0 \times 10^{-10\dagger}$	$4.7 \times 10^{-10\dagger}$
Dense sand and gravel											\dagger denotes assumed values

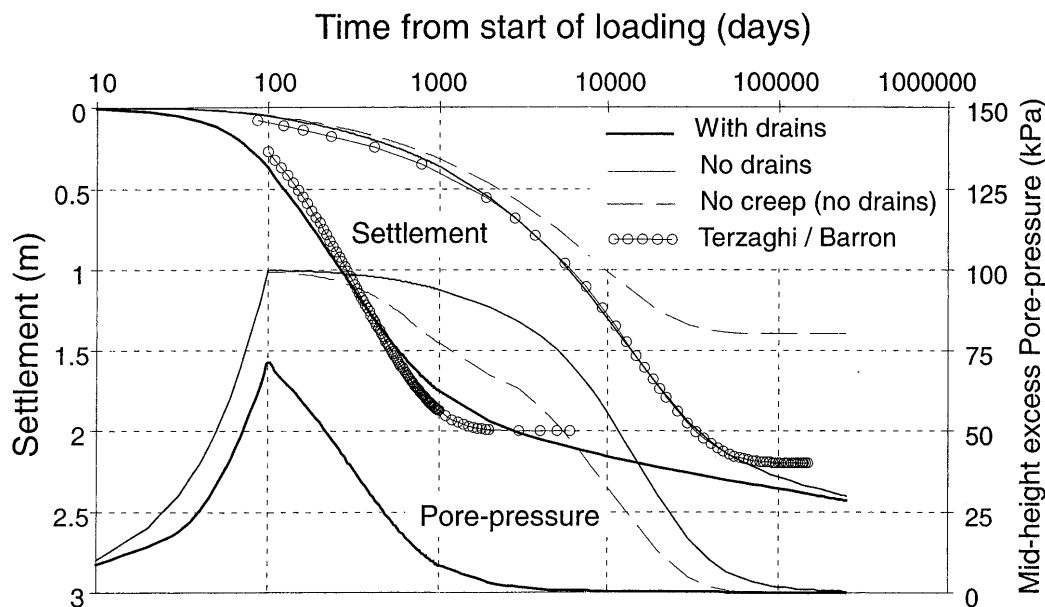


Fig. 7. Variation of predicted settlement and mid-height excess pore pressure with time under 100 kPa loading with and without vertical drains

try, pore pressure boundary conditions, permeability and state of the clays. The profile of vertical effective stress before filling is shown in Fig. 6, together with the final effective stress profile and the values of stress that were used to locate the RTL. The piezometric level at the top and bottom boundaries was taken to remain constant throughout consolidation at 0.8 m below initial ground level. The final effective stress increment is approximately 85 kPa since the submergence of the original ground surface below the water table reduced the applied stress. It may be seen that throughout the soft clay below the desiccated crust, the final effective stress is significantly larger than the RTL reference stress.

Initially a benchmark analysis was carried out to predict the long-term consolidation behaviour with vertical drainage alone under 100 kPa loading placed initially at 1 kPa/day. Using the EVP model type 2 described above, it was found that the long-term ground settlement would amount to nearly 2.5 m. The time-settlement behaviour and the excess pore pressure at mid-height are shown in Fig. 7. These indicate that the time for primary consolidation, indicated by the intersection of the linear portions of the logarithmic time-settlement plot and the dissipation of excess pore pressure, is around 35000 days (70 years). The very long consolidation time is due to the long drainage path as well as the combination of low permeability and high compressibility of the clay.

At this stage an analysis was also carried out to explore the significance of not modelling creep. This was carried out with the stress-strain behaviour defined using a curved normal consolidation line (NCL) coincident with the RTL for model 2 at each depth. As expected the magnitude of the long term settlement was much smaller at 1.4 m. The change of settlement and excess pore pressure at mid-height with time are shown in Fig. 7 alongside those using the EVP model, and it may be seen that the

Table 2. Predicted settlements after 250000 days under 100 kPa applied loading

Model	Without creep	With creep
1. (Yin and Graham, 1996)	1.44 m	2.56 m
2. (based on Butterfield, 1979)	1.40 m	2.41 m
3. (based on Den Haan, 1992)	1.29 m	2.21 m

creep increases both the magnitude of the long-term settlement and the time for primary consolidation by about 70%. The waviness of the pore pressure decay curve results from the change in stiffness as the clay passes through yield.

Analyses were then carried out to explore the use of the other EVP models type 1 and 3. These showed very similar time-settlement behaviour to that with model 2, with the smallest long-term settlement obtained using model 3 which uses the RTL with the greatest curvature. The long-term settlements for all these analyses are given in Table 2.

Next the effect of installing vertical drains prior to filling was considered. Free strain analyses were carried out using the EVP model 2 assuming a drain of effective diameter 100 mm to be at the centre of a unit cell 2 metres in diameter, with a smear zone of diameter 200 mm. In the smear zone the horizontal permeability was reduced to be equal to the vertical permeability of the undisturbed clay. The time-settlement behaviour and pore pressure decay are also shown in Fig. 7, and it may be seen that the magnitude and time for primary consolidation are reduced to about 1.9 m after around 1000 days (3 years). However in the long term the settlement increases to equal that calculated for the clay without vertical drains. A comparison between the free and equal strain analyses showed that the results were very similar.

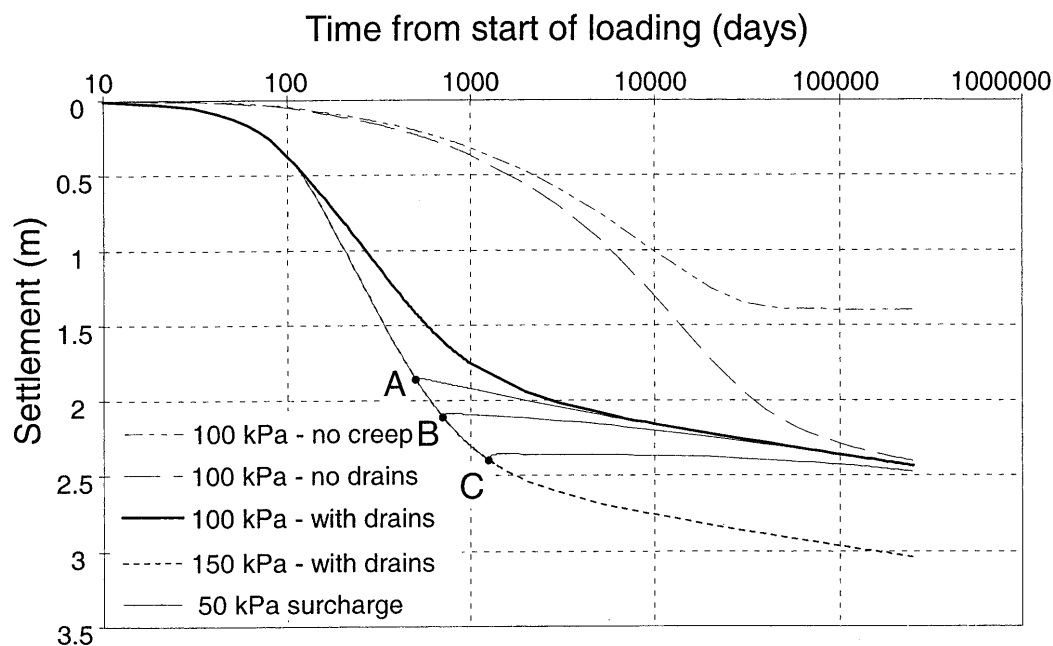


Fig. 8. Predicted time-settlement behaviour under 100 kPa loading showing effectiveness of temporary surcharge

Finally, the effect of placing a temporary 50 kPa surcharge in conjunction with the vertical drains was considered. First the effect of an indefinite 150 kPa loading was analysed using the EVP model 2 and a long-term settlement of 3 m was predicted. Analyses were then undertaken to examine the effects of removing the surcharge after 1, 1½ and 3 years. Figure 8 shows the time-settlement behaviour⁴ and the effectiveness of the surcharge may be assessed readily. It was found that when the surcharge was removed after 1 year (point A in Fig. 8) there were negligible residual excess pore pressures at mid-height. However after a short period of swelling, significant creep settlements resumed almost immediately (at a rate of nearly 70 mm/year). The profile of effective stress midway between the drains just before unloading is shown in Fig. 6, which confirms that the stresses at that time exceeded the final stresses (after surcharge removal) at all depths. The varying creep parameters result in a profile rather different from the normal isochrone shape. Leaving the surcharge in place for 1½ years (point B in Fig. 8) reduced the rate of settlement to 10 mm/year six months after removing the surcharge. After 3 years surcharge (point C) creep was almost eliminated (maximum subsequent settlement rate was 0.5 mm/year).

DISCUSSION

Stress Path during Consolidation

An important finding of this study is that the magnitude of the *total* long term settlement is independent of the drainage conditions. However the magnitude of the

⁴The progress of settlement was a little slower than that shown in Fig. 4 of Nash and Ryde (2000) where a smaller reduction of permeability with void ratio was assumed (equivalent to $C_k=1$).

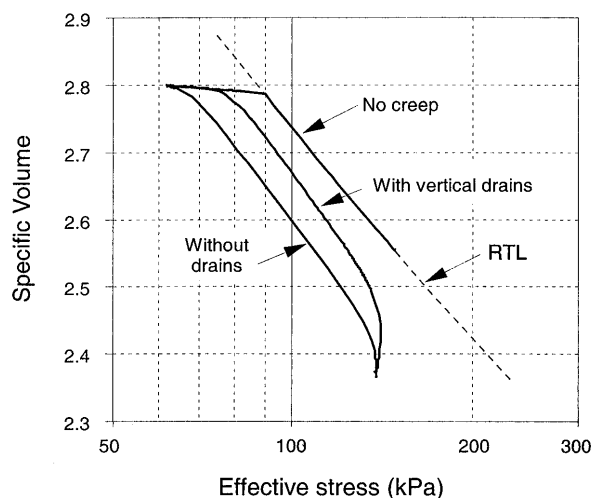


Fig. 9. Change of soil state under 100 kPa loading for different drainage conditions, with and without creep

primary consolidation settlement is not independent of the time for primary consolidation, with quicker consolidation resulting in smaller settlements. This may be understood if the change of soil state during consolidation is examined.

It is axiomatic that the stress-strain paths predicted by the EVP model are dependant on the drainage conditions (Hypothesis B referred to earlier). Longer drainage paths result in slower strain rates and larger creep strains; the slower the consolidation, the further the path lies below the RTL. Inherently field and laboratory stress-strain behaviours are different. This is illustrated in Fig. 9, which shows the RTL for this element, and the variation of void ratio and effective stress during consolidation for a soil element halfway down the soil profile for the anal-

yses with and without creep and vertical drains. The RTL_2 approximates to the 24-hour points in a laboratory oedometer test. With the non-creep model the field path follows the NCL (*i.e.* RTL_2) by definition. With the EVP model the field paths lie well below the RTL_2 , and their position, and the magnitude of the apparent yield stress, are dependent on the drainage conditions.

The implication of this is that analyses that ignore the creep behaviour of the clay would tend to under-predict the magnitude and duration of primary consolidation settlement.

Effectiveness of Surcharge

The EVP isotache models used here are able to predict many aspects of consolidation behaviour relevant to reclamation projects. In particular they are useful in predicting how long surcharge should be maintained to reduce creep after unloading to acceptable rates. The study above shows clearly that surcharging should be continued long enough to achieve the settlement that would occur in the long-term without surcharge, a criterion that may be hard to fulfil in practice.

Parametric studies may readily be carried out with procedures such as BRISCON to explore different scenarios. However it must be recognised that the models assume that the creep rate is only dependent on the current stress and void ratio, and that the value of ψ^* (or ψ) remains constant at large times, assumptions whose validity are uncertain (Yin, 1999). Daily load increments in IL consolidation tests only provide creep data under sustained loading for relatively short times, and special extended testing would be needed to establish behaviour on unloading definitively.

The simple isotache model can actually be used to make an estimate of the effect of removing a surcharge without resort to a numerical procedure. With reference to Fig. 2, at a given strain, reduction of effective stress from σ'_1 to σ'_2 (say from point C to E), results in a reduced creep rate and increased equivalent times. If Eqs. (5) and (9) are combined and $t_e \gg t_0$, the ratio of the creep strain rates may be approximated by:

$$\frac{\dot{\epsilon}_2}{\dot{\epsilon}_1} \approx \frac{t_{e1}}{t_{e2}} \approx \left(\frac{\sigma'_2}{\sigma'_1} \right)^{\lambda^*/\psi^*} \quad (17)$$

Equation (17) may be used to provide an estimate of the reduction of creep rate when a surcharge is removed using data from field instrumentation. This may be illustrated using the data from the study above, for example by considering the effect of removing surcharge after 1 year (point A in Fig. 8). The profile of effective stress before surcharge removal is first compared with that in the long term (Fig. 6). Dividing the soft clay into layers, the ratios of effective stresses are computed for the centre of each layer, and Eq. (17) is used to calculate the reduction in average creep rate for each layer, and thus for the whole profile. Such calculations have shown that when the surcharge is removed, the average creep rate after pore pressure equilibration would reduce to around 30% of its previous value. This compares with a reduction of

settlement rates to 11% of its previous value calculated using BRISCON, but some of the settlement occurring prior to unloading arises from pore pressure dissipation rather than creep. A better comparison is obtained when surcharge is removed after $1\frac{1}{2}$ and 3 years; Eq. (17) implies that creep rates are reduced to 3.5% and 0.4% of their previous values, which compare favourably with 3% and 0.5% obtained from BRISCON. Such agreement between BRISCON and Eq. (17) for surcharge removal after $1\frac{1}{2}$ and 3 years is expected, since by then the excess pore pressures have almost completely dissipated. At earlier times the simple approach using Eq. (17) underestimates the reduction of settlement rate achieved, which in practice would generally be conservative.

Back-Analysis of Time-Settlement Plots

Although the EVP model is very different from the linear elastic behaviour assumed in conventional analysis, it is interesting to compare the time-settlement behaviour during primary consolidation with that predicted under a loading of 100 kPa with and without vertical drains using conventional analyses. In the absence of vertical drains, a reasonable match of the time-settlement behaviour has been obtained with a standard consolidation analysis (Terzaghi, 1943) as shown in Fig. 7. In this analysis a constant coefficient of consolidation c_v of $0.8 \text{ m}^2/\text{year}$ was used, together with a maximum settlement of 2.2 m (corresponding to that at the end of primary consolidation in the EVP analysis). For analyses with vertical drains the time-settlement behaviour was predicted using the theory of Barron (1948) for which a constant horizontal coefficient of consolidation c_r of $1.2 \text{ m}^2/\text{year}$ and a maximum settlement of 2 m were assumed. Here the match is not so good (*see* Fig. 7) perhaps partly due to the contribution of vertical flow to the consolidation. The ratio of the c_r to the c_v found above from back-analysis is consistent with the average permeability ratio k_r/k_z of 1.5. In these calculations the time origin was assumed

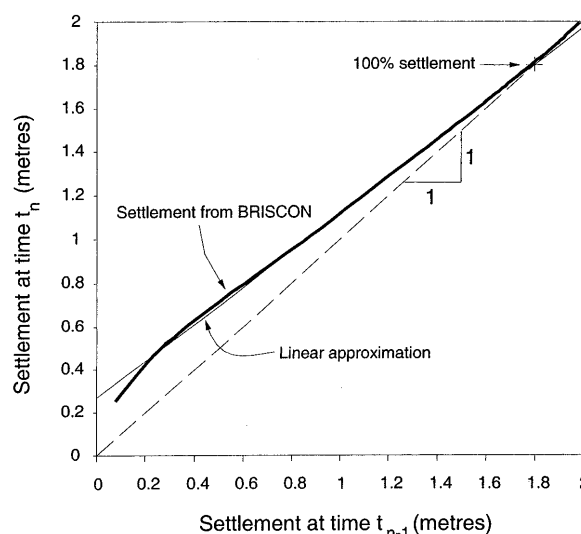


Fig. 10. Asaoka's plot of settlement under 100 kPa—with vertical drains

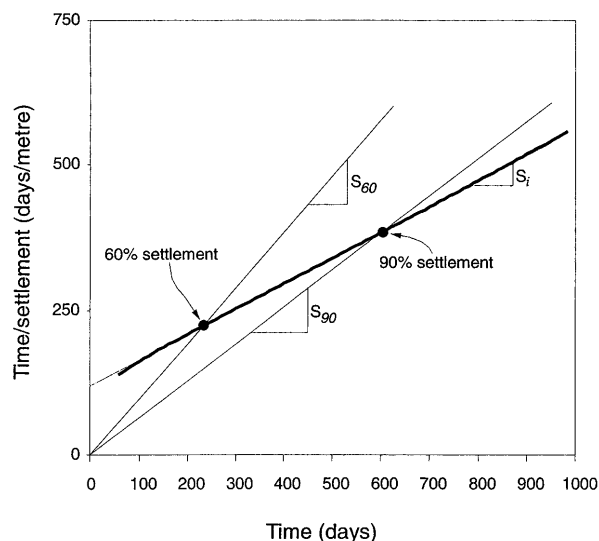


Fig. 11. Hyperbolic plot of settlement under 100 kPa—with vertical drains

to be halfway through the period of load application but data are plotted against the time from start of loading.

It is common practice to use field observations to explore the progress of consolidation using either Asaoka's method (Asaoka, 1978) or a hyperbolic plot (Tan, 1995; Tan and Chew, 1996). The present study provides an opportunity to examine the behaviour predicted by the EVP analysis in this way. The settlement data at equal time intervals Δt obtained from the EVP analysis with vertical drains has been plotted in the manner of Asaoka in Fig. 10. In this procedure settlement at time t_n is plotted against that at the previous time $t_{n-1} = t_n - \Delta t$, and this is expected to show a linear relationship. The plot in Fig. 10 shows curvature characteristic of settlement influenced by creep making it hard to select the most appropriate linear portion, but extrapolation of the linear portion here to intersect with the 1:1 line suggests a final settlement of 1.8 m. A radial coefficient of consolidation c_r of $1.65 \text{ m}^2/\text{year}$ has been calculated from the slope of the linear relationship using Eq. (22) of Holtz et al. (1991), but this value is very sensitive to the linear portion chosen.

In the hyperbolic method the ratio of elapsed time to settlement is plotted against time as shown in Fig. 11. Here the slope of the linear portion S_i is used in the prediction of the times for 60% and 90% consolidation and the magnitude of the settlement at the end of primary consolidation. The value of final settlement was calculated to be 1.74 m, and ignoring any effects of vertical flow the radial coefficient of consolidation c_r was calculated to be 1.63 and $1.57 \text{ m}^2/\text{year}$ for 60% and 90% consolidation respectively.

The settlement at the end of primary consolidation predicted by BRISCON is about 2 m, so it appears that settlement is under-predicted by these observational methods by more than 10%. The long-term settlement is of course even greater due to creep. The values of

coefficient of consolidation derived from the various back-analyses may be compared with values from laboratory tests. Nash et al. (1992) quote values of c_v for Bothkennar clay of about $10 \text{ m}^2/\text{year}$ at in-situ stress levels, but reducing to $1.0 \text{ m}^2/\text{year}$ at stresses four times higher when the clay has passed yield. Assuming an average permeability ratio k_r/k_z of 1.5 as before, the corresponding values of c_r are $15 \text{ m}^2/\text{year}$ reducing to $1.5 \text{ m}^2/\text{year}$. The large reduction arises from the non-linearity of the clay, together with the gradual change of its permeability with void ratio. It is satisfactory but perhaps fortuitous that the lower values are similar to the values obtained from the back-analyses. It is clearly difficult to predict the rate of consolidation reliably using conventional linear analyses and laboratory data.

CONCLUSIONS

The consolidation of soft soils accelerated by vertical drains frequently presents difficulties to designers of embankments and reclamation schemes over soft clays if there is significant creep. The elastic visco-plastic constitutive model developed here reproduces many features of soft clay behaviour commonly observed in the field and laboratory, and provides a helpful framework for the interpretation of data from high quality oedometer tests and field instrumentation. The incorporation of this one-dimensional EVP model in the finite difference procedure BRISCON enables predictions to be made for full-scale problems. Parametric studies may be undertaken where there is uncertainty over soil properties such as permeability and creep parameters, the extent of the smear zone and the effects of drain resistance. The case study presented here has illustrated the application of the model to the analysis of a full-scale problem involving soft clay exhibiting creep.

A significant aspect of the EVP model is that the creep strain rate depends only on the current state of the soil. This enables predictions to be made of behaviour after removal of a surcharge without resort to empirical methods. While simple hand calculations may be made to assess surcharge effectiveness where primary consolidation occurs quickly, the BRISCON procedure facilitates design to reduce long-term secondary settlements even if primary consolidation is not complete before a surcharge is removed.

Analysis of the data using Asaoka's method and the hyperbolic method resulted in under-prediction of the magnitude of primary consolidation settlements by at least 10%. These methods yielded coefficients of consolidation which were consistent with the values obtained in laboratory tests at high stress levels, but it appears that the use of simplified methods of analysis which ignore creep are not ever likely to result in reliable predictions of rate and magnitude of consolidation settlements.

ACKNOWLEDGEMENTS

The initial development of the BRISCON procedure

was undertaken by Dr. S. J. Ryde (formerly of Bristol University) who was sponsored by the Engineering and Physical Sciences Research Council. The author undertook further developments while seconded to Richard Davies Associates under the Royal Academy of Engineering Industrial Secondment Scheme.

NOTATION

b	index for power function defining reference time line for EVP model 3
c_v, c_r	vertical and horizontal coefficients of consolidation $k_z/\gamma_w m_v, k_r/\gamma_w m_v$
C_α	logarithmic creep function with respect to void ratio
C_c	compression index
e	void ratio
k_z, k_r	vertical and horizontal coefficients of permeability of soil
m_v	coefficient of volume compressibility
S_i, S_{60}	slope of linear segment of hyperbolic plot and slope for finding 60% consolidation
t, t_e	time and equivalent time
t_0	parameter used to determine strain rate on reference time line
u, \bar{u}, u_{ss}	pore pressure, excess pore pressure, steady-state pore pressure
v, v_0	specific volume, specific volume at zero strain
v_1, v_2, v_3	values of specific volume for fixing reference time lines
γ_w	unit weight of water
$\epsilon, \bar{\epsilon}$	engineering strain, natural strain
κ, λ, ψ	logarithmic material parameters for elastic and stress-dependent plastic strains and creep for EVP model 1
$\kappa^*, \lambda^*, \psi^*$	logarithmic material parameters for elastic and stress-dependent plastic strains and creep for EVP model 2
σ, σ'	vertical total and effective stresses
$\sigma'_1, \sigma'_2, \sigma'_3$	values of effective stress for fixing reference time lines
<i>Superscripts and Subscripts</i>	
e, ep, tp	instantaneous (elastic), stress-dependent plastic and time-dependent plastic

REFERENCES

- Asaoka, A. (1978): Observational procedure of settlement predictions, *Soils and Foundations*, **18** (4), 87-101.
- Barron, R. A. (1948): Consolidation of fine-grained soils by Drain Wells, *Trans. ASCE*, **113**, 718-754.
- Bjerrum, L. (1967): Engineering geology of Norwegian normally-consolidated clays, Seventh Rankine Lecture, *Géotechnique*, **17** (2), 81-118.
- Bjerrum, L. (1972): Embankments on soft ground, State of the Art Report, *Proc. Spec. Conf. on Performance of Earth and Earth-Supported Structures*, Purdue Univ., ASCE, **1**, 1-54.
- Butterfield, R. (1979): A natural compression law for soils (an advance on e -log p'), *Géotechnique*, **29** (4), 469-480.
- Den Haan, E. J. (1992): The formulation of virgin compression in soils, *Géotechnique*, **42** (3), 465-484.
- Den Haan, E. J. (1996): A compression model for non-brittle soft clays and peat, *Géotechnique*, **46** (1), 1-16.
- Garlanger, J. E. (1972): Consolidation of soils exhibiting creep under constant effective stress, *Géotechnique*, **22** (1), 71-78.
- Géotechnique (1992): Bothkennar soft clay test site: characterisation and lessons learned, Symp. in Print, *Géotechnique*, **42** (2), 161-378.
- Hansbo, S. (1981): Consolidation of fine-grained soils by prefabricated drains, *Proc. 10th Int. Conf. on SMFE, Stockholm.*, **3**, 677-682.
- Hight, D. W., Bond, A. J. and Legge, J. D. (1992): Characterisation of the Bothkennar clay: an overview, *Géotechnique*, **42** (2), 303-348.
- Holtz, R. D., Jamiolkowski, M., Lancellotta, R. and Pedroni, R. (1991): *Prefabricated Vertical Drains: Design and Performance*, CIRIA Ground Engrg. Report: Ground Improvement, Butterworth-Heinemann Ltd., Oxford.
- Jamiolkowski, M., Lancellotta, R. and Wolski, W. (1983): Precompression and speeding up consolidation, General Report to Spec. Session 6, *8th Eur. Conf. on SMFE, Helsinki*, **3**, 1201-1226.
- Johnson, S. J. (1970): Precompression for improving foundation soils, *J. Soil Mech. and Found. Div., ASCE*, **96** (SM1), 111-144.
- Kabbaj, M., Oka, F., Leroueil, S., and Tavenas, F. (1986): Consolidation of natural clays and laboratory testing, In *Consolidation of Soils: Testing and Evaluation*, (eds. by Yong, R. N. and Townsend, F. C.), ASTM STP 892, 71-103.
- Ladd, C. C., Foott, R., Ishihara, K., Schlosser, F. and Poulos, H. G. (1976): Stress-deformation and strength characteristics: State-of-the-art report, *Proc. 9th Int. Conf. on SMFE, Tokyo*, **2**, 421-494.
- Lee I. K., White W. and Ingles, O.G. (1983): *Geotech. Engrg.*, Pitman.
- Leroueil, S. (1988): Recent developments in consolidation of natural clays, 10th Can. Geotech. Colloquium. *Can. Geotech. J.*, **25** (1), 85-107.
- Magnan, J.-P., Baghery, S., Brucy, M. and Tavenas, F. (1979): Etude numérique de la consolidation unidimensionnelle en tenant compte des variations de la perméabilité et de la compressibilité du sol, du fluage et de la non-saturation, *Bulletin de Liaison des Laboratoires des Ponts et Chaussées*, **103**, 83-94.
- Mesri, G. and Choi, Y. K. (1985a): The uniqueness of the end-of-primary (EOP) void ratio-effective stress relationship, *Proc. 11th Int. Conf. on SMFE, San Francisco*, **2**, 587-590.
- Mesri, G. and Choi, Y. K. (1985b): Settlement analysis of embankments on soft clays, *J. Geotech. Engrg., ASCE*, **111** (GT4), 441-464.
- Mesri, G. and Godlewski, P. M. (1977): Time- and Stress-compressibility interrelationship, *J. Geotech. Engrg., ASCE*, **103** (GT5), 417-429.
- Mesri, G., Lo, D. O. K. and Feng, T. W. (1994): Settlement of embankments on soft clays, *Vertical and Horizontal Deformations of Foundations and Embankments*, ASCE, Geot. Spec. Pub., (40), 8-55.
- Murray, R. T. (1971): Embankments constructed on soft foundations: settlement study at Avonmouth, Report LR 419, Road Research Laboratory, Crowthorne, Berks, UK.
- Nash, D. F. T., Powell, J. J. M. and Lloyd, I. M. (1992): Initial investigations of the soft clay test bed site at Bothkennar, *Géotechnique*, **42** (2), 163-182.
- Nash, D. F. T. and Ryde, S. J. (1999): Modelling the effects of surcharge to reduce long term settlement of an embankment on soft alluvium, In *Geotech. Engrg. for Transportation Infrastructure*, (eds. Barends et al.) *Proc. 12th Eur. Conf. on SMGE, Amsterdam*, **3**, 1555-1561.
- Nash, D. F. T. and Ryde, S. J. (2000): Modelling the effects of surcharge to reduce long term settlement of reclamations over soft clays, *Int. Symp. on Coastal Geotech. Engrg. in Practice*, Yokohama Sep. 2000, 483-488.
- Nash, D. F. T. and Ryde, S. J. (2001): Modelling the consolidation of compressible soils subject to creep around vertical drains, *Géotechnique*, **51** (4), 257-273.
- Nash, D. F. T., Sills, G. C. and Davison, L. R. (1992): One-dimensional consolidation testing of soft clay from Bothkennar, *Géotechnique*, **42** (2), 241-256.
- Olsen, R. E. and Ladd, C. C. (1974): One-dimensional consolidation problems, *J. Geotech. Engrg., ASCE*, **105** (GT1), 11-30.
- Olsen, R. E., Daniel, D. E. and Liu, T. K. (1974): Finite difference analysis for sand drain problems, *Proc. Conf. on Analysis and Design in Geotech. Engrg.*, ASCE, **1**, 85-110.
- Onoue, A. (1988): Consolidation of multi-layered anisotropic soils by vertical drains with well resistance, *Soils and Foundations*, **28** (3), 75-90.
- Reece, G. (1986): Microcomputer modelling by finite differences,

Macmillan, London.

- 34) Richart, F. E. (1959): Review of the theories for sand drains, *Trans. ASCE*, **124**, 709-739.
- 35) Ryde, S. J. (1997): The performance and back-analysis of embankments on soft estuarine clay, PhD Thesis, University of Bristol.
- 36) Suklje, L. (1957): The analysis of the consolidation process by the isotache method, *Proc. 4th Int. Conf. on SMFE*, **1**, 200-206.
- 37) Tan, S. A. (1995): Validation of hyperbolic method for settlements in clay with vertical drains, *Soils and Foundations*, **35** (1), 101-113.
- 38) Tan, S. A. and Chew, S.-H. (1996): Comparison of the hyperbolic and Asaoka observational methods of monitoring consolidation with vertical drains, *Soils and Foundations*, **36** (3), 31-42.
- 39) Tatsuoka, F., Uchimura, T., Hayano, K., Di Benedetto, H., Koseki, J. and Siddiquee, M. S. A. (1999): Time-dependent deformation characteristics of stiff geomaterials in engineering practice, *Proc. 2nd Int. Symp. on Pre-failure Deformation Characteristics of Geomaterials*, Turin, Balkema.
- 40) Tavenas, F., Leblond, P., Jean, P. and Leroueil, S. (1983): The permeability of natural soft clays. Part II: Permeability characteristics, *Can. Geotech. J.*, **20** (4), 645-660.
- 41) Taylor, D. W. (1948): *Fundamentals of Soil Mechanics*, Chapman and Hall, London and Wiley, New York.
- 42) Taylor, D. W. and Merchant, W. (1940): A theory of clay consolidation accounting for secondary compression, *Journ. Math. Phys.*, **19** (3), 167-185.
- 43) Terzaghi, K. (1943): *Theoretical Soil Mechanics*, Chapman and Hall, London and Wiley, New York.
- 44) Yin, J.-H. (1999): Non-linear creep of soils in oedometer tests, *Géotechnique*, **49** (5), 699-707.
- 45) Yin, J.-H. and Graham, J. (1989): Viscous-elastic-plastic modelling of one-dimensional time-dependent behaviour, *Can. Geotech. J.*, **26** (2), 199-209.
- 46) Yin, J.-H. and Graham, J. (1994): Equivalent times and one-dimensional elastic visco-plastic modelling of time-dependent stress-strain behaviour of clays, *Can. Geotech. J.*, **31** (1), 42-52.
- 47) Yin, J.-H. and Graham, J. (1996): Elastic visco-plastic modelling of one-dimensional consolidation, *Géotechnique*, **46** (3), 515-527.

APPENDIX

Relation between the Parameters for Model 1 and Model 2

The equations of the two reference time lines are:

$$v^{ep} = v_1^{ep} - \lambda \ln \left(\frac{\sigma'}{\sigma_1^{ep}} \right) \quad \text{for model 1} \quad (\text{A.1a})$$

$$\ln(v^{ep}) = \ln(v_2^{ep}) - \frac{\lambda^*}{v_0} \ln \left(\frac{\sigma'}{\sigma_2^{ep}} \right) \quad \text{for model 2.} \quad (\text{A.1b})$$

Coincidence of the two reference time lines at the common state (σ_1^{ep} , v_1^{ep}) may be achieved by choosing (σ_2^{ep} , v_2^{ep}) to be coincident with (σ_1^{ep} , v_1^{ep}) and matching the slope of the two lines. The slopes of the lines at this state are given by:

$$\frac{\partial v^{ep}}{\partial \sigma} = -\frac{\lambda}{\sigma_1^{ep}} \quad \text{for model 1} \quad (\text{A.2a})$$

$$\frac{\partial v^{ep}}{\partial \sigma} = -\frac{\lambda^* v_1}{v_0 \sigma_1^{ep}} \quad \text{for model 2.} \quad (\text{A.2b})$$

Equating these leads to:

$$\lambda^* = \frac{\lambda v_0}{v_1}. \quad (\text{A.3})$$

Similar reasoning leads to the expression:

$$\kappa^* = \frac{\kappa v_0}{v_1}. \quad (\text{A.4})$$

The creep strains are obtained using the expressions for rate of change of specific volume:

$$\frac{\partial v^{tp}}{\partial t} = -\psi \ln \left(1 + \frac{t_c}{t_0} \right) \quad \text{for model 1} \quad (\text{A.5a})$$

$$\frac{\partial v^{tp}}{\partial t} = -\frac{v\psi^*}{v_0} \ln \left(1 + \frac{t_c}{t_0} \right) \quad \text{for model 2.} \quad (\text{A.5b})$$

Equating these at the common point on the RTL leads to:

$$\psi^* = \frac{\psi v_0}{v_1}. \quad (\text{A.6})$$

Choice of Reference State for Model 3

In model 3 the specific volume is related to its value at a reference state (σ_3^{ep} , v_3^{ep}) given by:

$$v^{ep} = v_3^{ep} (\sigma' - (\sigma_3^{ep} - 1))^{-b} \quad (\text{A.7a})$$

or

$$\ln(v^{ep}) = \ln(v_3^{ep}) - b \ln(\sigma' - (\sigma_3^{ep} - 1)). \quad (\text{A.7b})$$

The RTL for Model 1 is given by Eq. (A.1a). Coincidence of these reference time lines at the common state (σ_1^{ep} , v_1^{ep}) may be achieved as before by matching the slope and position of the lines. The slopes of the lines at this state are given by:

$$\frac{\partial v^{ep}}{\partial \sigma} = -\frac{\lambda}{\sigma_1^{ep}} \quad \text{for model 1} \quad (\text{A.8a})$$

$$\frac{\partial v^{ep}}{\partial \sigma} = \frac{-bv_1^{ep}}{\sigma_1^{ep} - (\sigma_3^{ep} - 1)} \quad \text{for model 3.} \quad (\text{A.8b})$$

Equating these leads to:

$$\sigma_3^{ep} = \sigma_1^{ep} \left(1 - \frac{bv_1^{ep}}{\lambda} \right) + 1. \quad (\text{A.9})$$

Substituting this value into Eq. (A.7a) leads to:

$$v_3^{ep} = v_1^{ep} \left(\frac{bv_1^{ep} \sigma_1^{ep}}{\lambda} \right)^{-b}. \quad (\text{A.10})$$

By inspection model 3 reduces to model 2 if:

$$b = \frac{\lambda^*}{v_0} = \frac{\lambda}{v_1}. \quad (\text{A.11})$$

The creep parameters for model 3 are related to those for model 1 in a similar manner but the derivation is more lengthy and will be presented elsewhere.